

Measurement of dislocation core distribution by digital processing of high-resolution transmission electron microscopy micrographs: a new technique for studying defects

This article has been downloaded from IOPscience. Please scroll down to see the full text article.

2000 J. Phys.: Condens. Matter 12 10313

(<http://iopscience.iop.org/0953-8984/12/49/334>)

View [the table of contents for this issue](#), or go to the [journal homepage](#) for more

Download details:

IP Address: 171.66.16.226

The article was downloaded on 16/05/2010 at 08:12

Please note that [terms and conditions apply](#).

# Measurement of dislocation core distribution by digital processing of high-resolution transmission electron microscopy micrographs: a new technique for studying defects

Sławomir Kret<sup>†</sup>, Paweł Dłużewski<sup>‡</sup>, Piotr Dłużewski<sup>†</sup> and Ewa Sobczak<sup>†</sup>

<sup>†</sup> Institute of Physics, PAS, Alca Lotników 32/46, 02-668 Warszawa, Poland

<sup>‡</sup> Institute of Fundamental Technological Research, PAS, ul. Świętokrzyska 21, 02-049 Warszawa, Poland

Received 28 September 2000

**Abstract.** A new technique for studying extended defects and dislocation networks is proposed. The approach, based upon the continuum theory of crystal defects, is employed for digital image processing of high-resolution transmission electron micrographs. The procedure starts with the geometric phase method for extracting the lattice distortion field near dislocation cores. Next, the dislocation core distribution (DCD) is recovered from the lattice distortion field. A so-obtained DCD field takes non-zero values only in disordered regions of the lattice. The accuracy of this method is investigated by mathematical integration of the dislocation field over core regions to find the in-plane components of the Burgers vectors. The proposed method is free of topological problems and can be used to study spatial configurations of complex defects in large crystal areas by using a fully automatic computer program. This approach is applied to investigate a network of misfit dislocations in the interfacial region of a GaAs/ZnTe/CdTe heterostructure.

## 1. Introduction

In recent years, several papers have been devoted to the measurement of lattice distortions from HRTEM micrographs [1–4]. These papers base their analysis on the assumption that lattice fringe spacings in HRTEM images give information on lattice distortions in the sample observed. Bierwolf *et al* [1] reported the measurement of one-dimensional strain fields in a pseudomorphic quantum well in the GaAs/GaInAs system. The method is based on the measurement of spacing between peaks in image darkness. Comparing the positions of maxima in layers to analogous ones in the substrate, the authors have determined the displacement field in the deformed crystal lattice. A similar method has been applied by Kret *et al* [2] to the mapping of the 2D long-range strain field in coherent GaAs/GaInAs islands. Another method, called the geometric phase method, has been developed by Hÿtch *et al* [3]. The method is free of topological problems of numbering lattice points in the reference and investigated areas. This method has been employed by Snoeck *et al* [4] to measure lattice distortions in the vicinity of misfit dislocations situated in the interfacial zone of the heteroepitaxial structure GaAs/GaSb.

In the present work, an approach based on the continuum field theory is employed to extract the shape and the dislocation core distribution (DCD) from HRTEM micrographs. The GaAs/ZnTe/CdTe highly mismatched heteroepitaxial system is used to demonstrate our approach.

## 2. Extraction of the lattice distortion tensor (LDT) from HRTEM micrographs

Our procedure for measuring dislocation core distribution starts with the reconstruction of distortion fields from HRTEM micrographs using the geometric phase method.

In the GaAs/ZnTe/CdTe system the 14.6% lattice mismatch between GaAs and ZnTe/CdTe is accommodated by a misfit dislocation network at the interface. A thick CdTe film was grown by molecular beam epitaxy (MBE) on the GaAs(100) Epiready substrate miscut towards [011] with a  $2^\circ$  disorientation. A 2 ML thick ZnTe intermediate layer was used to improve the quality of the epilayer. Cross-sectional specimens were prepared using the conventional grinding and argon-ion thinning technique with cooling by liquid nitrogen. The high-resolution electron microscopy was performed using a Philips CM 20 UT microscope operating at 200 kV with a point resolution of 0.19 nm. For imaging GaAs along the [110] zone axis an aperture of  $11 \text{ nm}^{-1}$  and nine beams (000,  $4 \times 111$ ,  $2 \times 220$ ,  $2 \times 200$ ) were used. Defocus values close to the Scherzer defocus ( $-43 \text{ nm}$ ) were chosen in order to obtain large zones of homogeneous contrast, white dots on black background, for both GaAs and CdTe. The thickness of the foil was uniform and estimated to be below 15 nm. A typical high-quality image of a GaAs/CdTe interface in the [110] projection is shown in figure 1. All misfit dislocations visible at the interface are Lomer dislocations. Their Burgers vectors have  $\frac{1}{2}[1\bar{1}0]$  components. The dislocation lines are in the interfacial plane and parallel to the electron beam. The core structures of all dislocations visible in figure 1 are mutually different. Moreover, their cores are significantly different from those of the Lomer dislocations on the (100) interfacial plane in GaAs/CdTe previously studied by McGibbon *et al* [5].

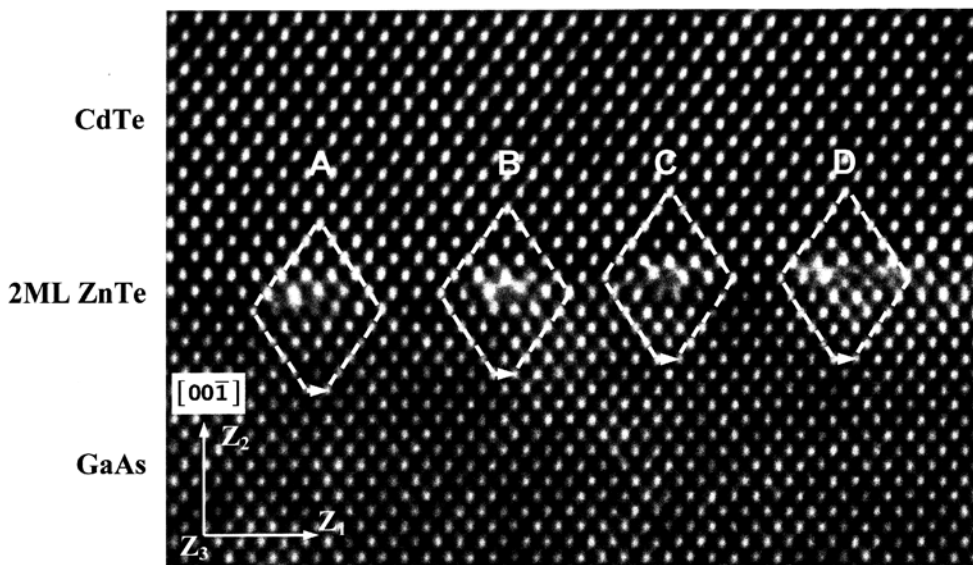


**Figure 1.** A high-resolution image of a GaAs/ZnTe/CdTe interface observed along the [110] projection. The Burgers circuit is drawn according to the SF/RH rule.

For image processing, the HRTEM image has been recorded in the form of a  $1024 \times 1024$  pixel matrix. The unit vectors  $z_1, z_2, z_3$  (basis vectors) in the orthonormal coordinate system  $\{z_k\}$  have been chosen as shown in figure 1. First the phase images  $P_{g_{111}}$  and  $P_{g_{\bar{1}\bar{1}\bar{1}}}$  were calculated for  $1\bar{1}\bar{1}$  and  $111$  image periodicity. A GaAs substrate free of dislocations was chosen as the reference. The lattice displacement  $\hat{u}(z_1, z_2)$  was calculated using the following

relations (see [3]):

$$P_{g_i}(z_1, z_2) = -2\pi g_i \cdot \widehat{\mathbf{u}}(z_1, z_2). \quad (1)$$

The two-dimensional distortion field  $\beta(z_1, z_2)$  shown in figure 2 has been determined by differentiation of the displacement field  $\widehat{\mathbf{u}}(z_1, z_2)$  using the following equations:

$$\beta = \begin{bmatrix} \beta_{11} & \beta_{12} \\ \beta_{21} & \beta_{22} \end{bmatrix} = \begin{bmatrix} \frac{\partial \widehat{u}_1}{\partial z_1} & \frac{\partial \widehat{u}_1}{\partial z_2} \\ \frac{\partial \widehat{u}_2}{\partial z_1} & \frac{\partial \widehat{u}_2}{\partial z_2} \end{bmatrix}. \quad (2)$$

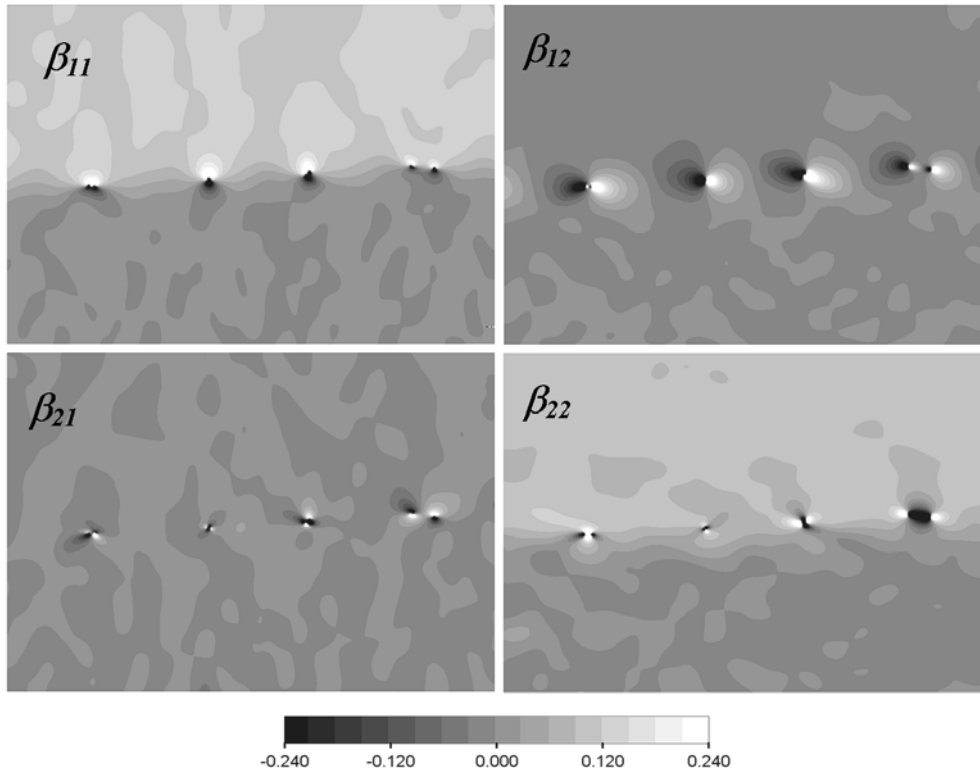


Figure 2. Distribution of the lattice distortion tensor  $\beta$ .

### 3. Dislocation core distribution and Burgers vector determination from the LDT

From the viewpoint of the dislocation theory (cf. [6]), the Burgers vector referred to the lattice spacings in the reference perfect-crystal lattice is described by the following dislocation distribution tensor:

$$\widetilde{\boldsymbol{\alpha}} \stackrel{\text{df}}{=} -\text{curl } \beta. \quad (3)$$

Consider the geometric meaning of the dislocation tensor. Let the Burgers circuit be drawn around the dislocation core in the deformed lattice. Making a local mapping to any chosen reference in the perfect lattice we find a non-closed circuit and the Burgers vector  $\mathbf{b}$  needed

to close it. Using the Stokes theorem, this local mapping has the following mathematical representation in the continuum theory of dislocations:

$$\widehat{\mathbf{b}} = - \int_{s_c} \widetilde{\boldsymbol{\alpha}} \, ds \quad (4)$$

where  $s_c$  is the cross-section region of the dislocation. The differential  $ds$  of the area vector is understood here as a product  $ds = \mathbf{n} \, ds$  where  $\mathbf{n}$  is the unit vector perpendicular to the cross-section while  $ds$  is a scalar element of dislocation core area. The geometric meaning of the tensorial measure  $\widetilde{\boldsymbol{\alpha}}$  can be also expressed in a differential form:

$$d\widehat{\mathbf{b}} = \widetilde{\boldsymbol{\alpha}} \, ds \quad (5)$$

relating the respective increase of the Burgers vector  $d\widehat{\mathbf{b}}$  to the area element  $ds$  of the dislocation core region. Using the two-dimensional field  $\beta(z_1, z_2)$  extracted from the HRTEM, the components  $\alpha_{12}$  and  $\alpha_{23}$  of the dislocation distribution tensor have been determined from

$$\widetilde{\alpha}_{13} = - \frac{\partial \beta_{12}}{\partial z_1} + \frac{\partial \beta_{11}}{\partial z_2} \quad (6)$$

$$\widetilde{\alpha}_{23} = - \frac{\partial \beta_{22}}{\partial z_1} + \frac{\partial \beta_{21}}{\partial z_2}. \quad (7)$$

The so-determined in-plane components of the tensorial field of the dislocation distribution take zero values over the whole region analysed except at the dislocation cores, where they form characteristic local peaks (figure 3). The peaks are surrounded by a zero-value field within an accuracy of  $10^{-6}$  times the densities reached at the peaks. By definition, the dislocation density tensor should uniquely determine the Burgers vector distribution over the space of the dislocation core. Integrating the components of  $\widetilde{\boldsymbol{\alpha}}$  over the whole dislocation core region, we can find the components of the Burgers vectors. According to (4) we find

$$\widehat{b}_1 = \int_{S_c} \widetilde{\alpha}_{13} n_3 \, ds \approx \sum_{i=1}^k \widetilde{\alpha}_{13} \Delta S_{\text{pxl}_i} \quad (8)$$

$$\widehat{b}_2 = \int_{S_c} \widetilde{\alpha}_{23} n_3 \, ds \approx \sum_{i=1}^k \widetilde{\alpha}_{23} \Delta S_{\text{pxl}_i} \quad (9)$$

where  $S_{\text{pxl}_i}$  denotes the area of the region occupied by the  $i$ th pixel. In digital image processing, the whole dislocation core has been divided into area elements corresponding to pixels, i.e.  $S_{\text{pxl}_i} = \sum_{i=1}^k \Delta S_{\text{pxl}_i}$ .

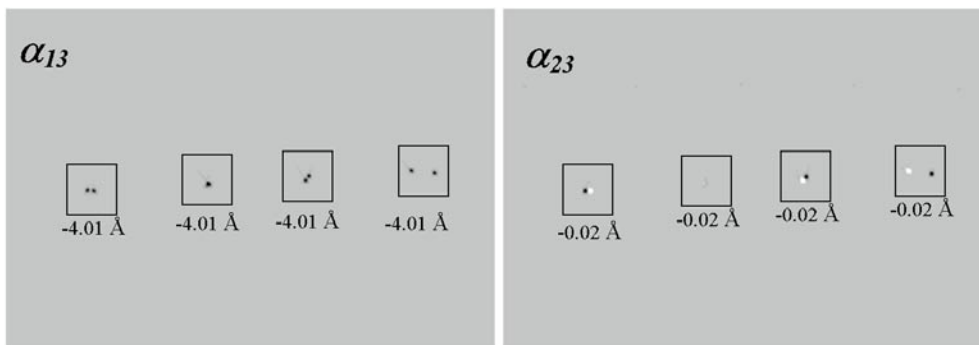


**Figure 3.** The tensorial distribution of the dislocation cores determined from the HRTEM micrograph (cf. figure 1).

As shown in figure 3, the dislocation core density tensor takes non-zero values only near the dislocation core and each single peak extension is about 0.5 nm. We can see that the calculated Burgers vector components are very close to the theoretical values for GaAs. All the dislocations have the same Burgers vector. The calculated Burgers vector components are very close to each other, but the distributions of the dislocation core densities are quite different. Dislocations A, C and D have clearly visible separations of  $\tilde{\alpha}_{13}$  into two positive symmetric maxima, but the field  $\tilde{\alpha}_{23}$  is split into a maximum and a minimum. Integrating these two dislocation density peaks separately, we obtain two Burgers vectors corresponding to in-plane components of two  $60^\circ$  dislocations. This agrees with the fact that a Lomer dislocation can be interpreted as two merged  $60^\circ$  elemental dislocations coming from different  $\{111\}$  planes. The core of dislocation B is more compact, so its  $\alpha_{13}$ -component has only one maximum and a near-zero value of the second component. The observed difference in the  $\tilde{\alpha}$ -distribution can be attributed to the differences in atomic structure of the dislocations cores caused by the local variation of the chemical composition. The zinc atoms could have migrated from the ZnTe monolayers to the cores and stabilized them. Another possible explanation for this dislocation core diversity is as arising from interactions between dislocations and interface steps which are present due to disorientation of the substrate used to grow the samples investigated.

#### 4. Conclusions and perspectives

The method applied gives a very high accuracy in determining the tensorial field of the dislocation distribution and Burgers vectors components. It is worth emphasizing that outside of dislocation cores, the tensor  $\tilde{\alpha}$  reaches zero values with an accuracy of  $10^{-6}$  of the values obtained in the core regions. In general, our procedure only gives information about the position of the maximum of the distortion, which is useful for determining the character of the dislocation core but not the atomic structure. For example, by extracting the continuum field  $\tilde{\alpha}$  for Lomer dislocations, it is easy to establish by precisely how much the centres of elemental  $60^\circ$  dislocations are separated from each other. More work will be necessary to correlate the atomic structure of the dislocation cores and the calculated distribution of the dislocation density tensor. The continuous tensorial fields of defect distributions are suited well to computer-aided recognition of the geometric parameters of lattice defects on the basis of HRTEM micrographs. The proposed technique provides the possibility of building a program for on-line computer-aided recognition of planar components of Burgers vectors during HRTEM observations.

#### Acknowledgments

The present work was partially funded by the State Committee for Scientific Research (KBN) in Poland under Grants No 7T07A 004 16 and No 2P03B 103 14. The sample was made at IF-PAS in Warsaw while the HRTEM investigation was carried out with the collaboration of LPS-ESPCI on the CM-20UT microscope at the Ecole Centrale de Paris.

#### References

- [1] Bierwolf R, Hohenstein M, Phillipp F, Brandt O, Crook G E and Ploog K 1993 *Ultramicroscopy* **49** 273
- [2] Kret S, Delamarre C, Laval J Y and Dubon A 1998 *Phil. Mag. Lett.* **77** 249
- [3] Hÿtch M J, Snoeck E and Kilaas R 1998 *Ultramicroscopy* **74** 131
- [4] Snoeck E, Warot B, Arduin H, Rocher A, Casanove M J, Kilaas R and Hÿtch M J 1998 *Thin Solid Films* **319** 157

- [5] McGibbon A J, Pennycook S J and Angelom J E 1995 *Science* **269** 519
- [6] Hirth J P and Lothem L 1982 *Theory of Dislocations* 2nd edn (New York: Wiley)
- [7] Cheng T T, Aindow A, Jones I P, Hails J E and Williams D J 1995 *J. Cryst. Growth* **154** 251
- [8] Dłużewski P 1996 *Mech. Mater.* **22** 23